High Dielectric Constant Polycarbonate/Nylon Multilayer Films Capacitors with Self-healing Capability

Zhenpeng Li,[†] Xinyue Chen,[†] Ci Zhang,[†] Eric Baer,[†] Deepak Langhe,[‡] Michael Ponting,[‡] Michael Brubaker,[§] Terry Hosking,[§] Ruipeng Li,[#] Masafumi Fukuto,[#] and Lei Zhu*[,†]

[†] *Department of Macromolecular Science and Engineering, Case Western Reserve University, Cleveland, Ohio 44106-7202, United States*

[‡] *PolymerPlus, LLC, 7700 Hub Parkway, Valley View, Ohio 44125, United States*

[§] *SBE, Inc., 81 Parker Road, Barre, Vermont 05641-9106 United States*

[#] *National Synchrotron Light Source II, Brookhaven National Laboratory, Upton, New York 11973, United States*

* Corresponding author, Email address: lxz121@case.edu (L. Zhu).

Keywords: Multilayer films, polycarbonate, *n*-nylons, dielectric properties, high temperature capacitors, self-healing

Abstract

With the fast development of high temperature metal oxide semiconductor field effect transistors for power electronics in electric vehicles, current state-of-the-art biaxially oriented polypropylene (BOPP) film capacitors need further improvement, because they have a temperature rating of only 85 °C without derating the voltage to maintain a long lifetime. If a high temperature polymer can replace BOPP without sacrificing the overall dielectric performance and cost, it is possible to remove the current water-cooling system for capacitors and significantly reduce the cost of the power electronic unit. In this work, we demonstrated new polycarbonate (PC)/nylon multilayer films (MLFs), which has a potential for even higher temperature rating because of the higher melting temperature for nylons (e.g., nylon-6). Structural and dielectric studies showed that these PC/nylon MLFs had a similar dielectric performance, such as dielectric constant, dielectric loss, and breakdown strength, as the PC/poly(vinylidene fluoride) PVDF MLFs, which were developed in the past. These PC/nylon MLFs could perform well up to 120 °C, which was limited by the glass transition temperature of PC at 145 °C. More intriguingly, packaged PC/nylon-12 MLF capacitors exhibited a self-healing capability, which had been difficult for packaged high temperature film capacitors. Because self-healing is such a fundamental requirement for polymer film capacitors, our PC/nylon MLFs offer a potential for next-generation high temperature and high energy density film capacitors.

Introduction

Power electronic inverters and electric motors are major components of the traction drives in electric vehicles (EVs), which hold the promise to lower greenhouse emission and pollution in heavily populated cities.[1] The DC-link capacitor is the largest capacitor in the traction drive system, interfacing between the DC/DC converter or battery and the DC/AC inverter. Its primary function is to support a DC network by smoothing DC input current and functioning as an energy buffer during load transients. Namely, it enables quick energy transfer into the insulated gate bipolar transistor (IGBT)-based or SiC-based inverter circuit, smooths out DC-bus voltage variation, and prevents ripple from interfering with the DC power source. Required by the integration of power electronics circuits, DC-link capacitors are tightly integrated with the semiconductor switches to minimize the commutation loop inductance and enable fast switching.

For DC-link capacitors in EVs, many technologies have been in competition, including ceramic capacitors,[2-3] supercapacitors,[4] electrolytic capacitors,[5] and polymer film capacitors.[6-7] Ceramic capacitors have high temperature capability; however, they are heavy (i.e., energy density per weight is low) and do not have the self-healing capability,[6-7] which is critical for long-life operation of capacitors. Super- or ultra-capacitors are promising for high energy density applications; however, they have high dielectric loss in the 10-40 kHz frequency range for DC-link capacitors.[8] Meanwhile, they are water- or solvent-based; therefore, they tend to dry out at high temperatures. Electrolytic capacitors, such as aluminum and tantalum capacitors, have high energy density; however, they cannot handle high ripple current required for DC-link capacitors at high voltages. Meanwhile, the aqueous electrolyte-based capacitors also tend to dry out at high temperatures. Polymer film capacitors have advantages of high ripple current, high voltage, low loss, and self-healing capability.[6-7] After years of practice, polymer film capacitors have been

proven to be the most suitable technology for high voltage, high temperature, and high ripple current power electronic systems used in EVs.[1, 9] For polymer film-based DC-link capacitors, current state-of-the-art technology is BOPP film capacitors.[6-7] The thinnest BOPP film thickness has reached as low as ~2.5 μm while not significantly sacrificing performance of breakdown strength and lifetime.[10] However, BOPP capacitors still occupy 1/3 of the volume and cost 1/3-1/2 the price of the power electronic unit. When temperature is above 85 °C, they have a 30-50% voltage derating due to deteriorated breakdown strength and lifetime of the films. Because of this temperature limit, BOPP DC-link capacitors need an external cooling system with 60-75 °C cooling water. This incurs additional costs to the entire power electronic system in EVs. Therefore, it is desirable to achieve high temperature performance and to miniaturize film capacitors via enhancing the energy density (i.e., to reduce the overall cost).

Table 1. Metrics Comparison between Monolithic Films and Multilayer Films.

	BOPP	BOPET	BOPEN	PPS	PC	COC	PEI	PVDF-MLFs
T_g (°C)	-15	75	120	90	145	180	215	-40 (PVDF)
T_m (°C)	165	260	270	285	-	-	-	175 (PVDF)
Dielect. const. (ε_r)	2.25	3.3	3.0	2.8	2.8	2.3	3.15	4-7
Dielect. loss (tanδ)	0.0003	0.003	0.001	0.0005	0.001	0.0003	0.005	<0.01
Minimum film thickness (μm)	2-3	0.7	1.0	1.2	3	>10	>10	3-12
Breakdown field (MV/m)	730	580	600	500	600	500	450	700-1000
U_e at breakdown (J/cm^3)	5.0	6.0	6.0	3.0	3.0	2.5	4.0	>13
Temperature (°C)	<80	<140	<140	<160	<120	<150	<150	up to 150

T_g: glass transition temperature, T_m: melting temperature, U_e: energy density at the film level, PET: poly(ethylene terephthalate), PEN: poly(ethylene 2,6-naphthalate), PPS: poly(phenylene sulfide), PC: polycarbonate, COC: cyclic olefin copolymers of ethylene/hydrogenated norbornene, PEI: polyetherimide, PVDF: poly(vinylidene fluoride).

Table 1 summarizes properties of potential high temperature monolithic films and poly(vinylidene fluoride) (PVDF)-based multilayer films (MLFs) developed at Case Western Reserve University (CWRU).[10-14] Polyester films include biaxially oriented poly(ethylene

terephthalate) (PET) and poly(ethylene naphthalate) (PEN) films.[15] They are relatively cheap and can be readily processed into films as thin as 1 μm thick. However, they are not suitable for EV DC-link capacitors simply because of their high dielectric losses at temperatures above 100-120 °C (i.e., above their glass transition temperatures, T_gs). Recently, DuPont Teijin Films developed a new type of PEN-based high temperature film, which can operate up to 150 °C.[16] Poly(phenylene sulfide) (PPS) is a good high temperature candidate, which can survive up to 160 °C.[10] However, the price for biaxially oriented PPS films (~3 μm) is astonishingly high, preventing it from entering the DC-link capacitor market. Polycarbonate (PC, no longer produced on a commercial scale), polysulfone (PSF), and cyclic olefin copolymers (COC, e.g., TOPAS®) films are mostly amorphous. Although they have relatively high T_gs, the biaxially oriented films exhibit significant shrinkage at temperatures above 120 °C. Poly(ether imide) (PEI, e.g., Ultem®) is still under development.[11] Despite its high cost, it has also been challenging to achieve thin (~3 μm) high quality capacitor-grade films.

From Table 1 and our recent perspective review,[17] we can see another significant problem for nearly all existing high temperature polymers, i.e., their dielectric constants are mostly smaller than 3.5 and thus the energy densities are not much higher than that of BOPP. Without increasing energy density, it is impossible to achieve lower costs than BOPP films without achieving significantly thinner (i.e., <1 μm) and higher breakdown strength/longer life dielectric films. To address this grand challenge, we have developed a unique MLF coextrusion technology to achieve high temperature capability and high energy density at the same time. By multilayering a high dielectric constant polymer (e.g., PVDF) with a high temperature, high breakdown/low loss polymer (e.g., PC or PSF), we have already achieved, at the film level, a high energy density (13 J/cm^3 at breakdown, i.e., 2.5 times that of BOPP) and low dielectric/hysteresis losses ($\tan\delta$ <0.005)

up to 120 °C.[14] The advantage of the MLF technology lies in the capability of achieving high temperature performance and high energy density simultaneously, as well as simple melt processing. This is different from the complicated processing of multilayer ceramic capacitors.[2-3]

In this work, we explore the opportunity of polyamides (PAs) or nylons as a new high dielectric constant polymer for multilayer capacitor films. To avoid ferroelectricity in odd-numbered nylons, we choose even-numbered *n*-nylons, such as nylon-6 and nylon-12, to multilayer with PC, because even-numbered nylons do not show significant ferroelectricity, especially at elevated temperatures.[18] Above the T_g, even-numbered nylons are primarily paraelectric and the amorphous phase exhibits a high dielectric constant (>10) due to the dipolar polarization of the amorphous amide dipoles. PC/nylon 50/50 (vol./vol.) 33-layer (33L) films with good layer integrity are successfully fabricated. The dielectric performance, in terms of breakdown strength, electric displacement-electric field (D-E) loop hysteresis loss, and discharged energy density, is compared between PC/nylon and PC/PVDF MLFs. It is observed that dielectric constants and energy densities are similar for PC/nylon and PC/PVDF MLFs, when the temperature is above 75 °C. After metallization and winding of PC/nylon-12 MLFs into ~22 μF capacitors, self-healing is observed when the PC/nylon-12 MLF capacitor is under an electrical stress up to 2000 V. This is in drastic contrast to the PC/PVDF MLF capacitors, which are difficult to show the self-healing capability. From this study, we conclude that PC/nylon MLFs could be promising for future high temperature capacitor applications.

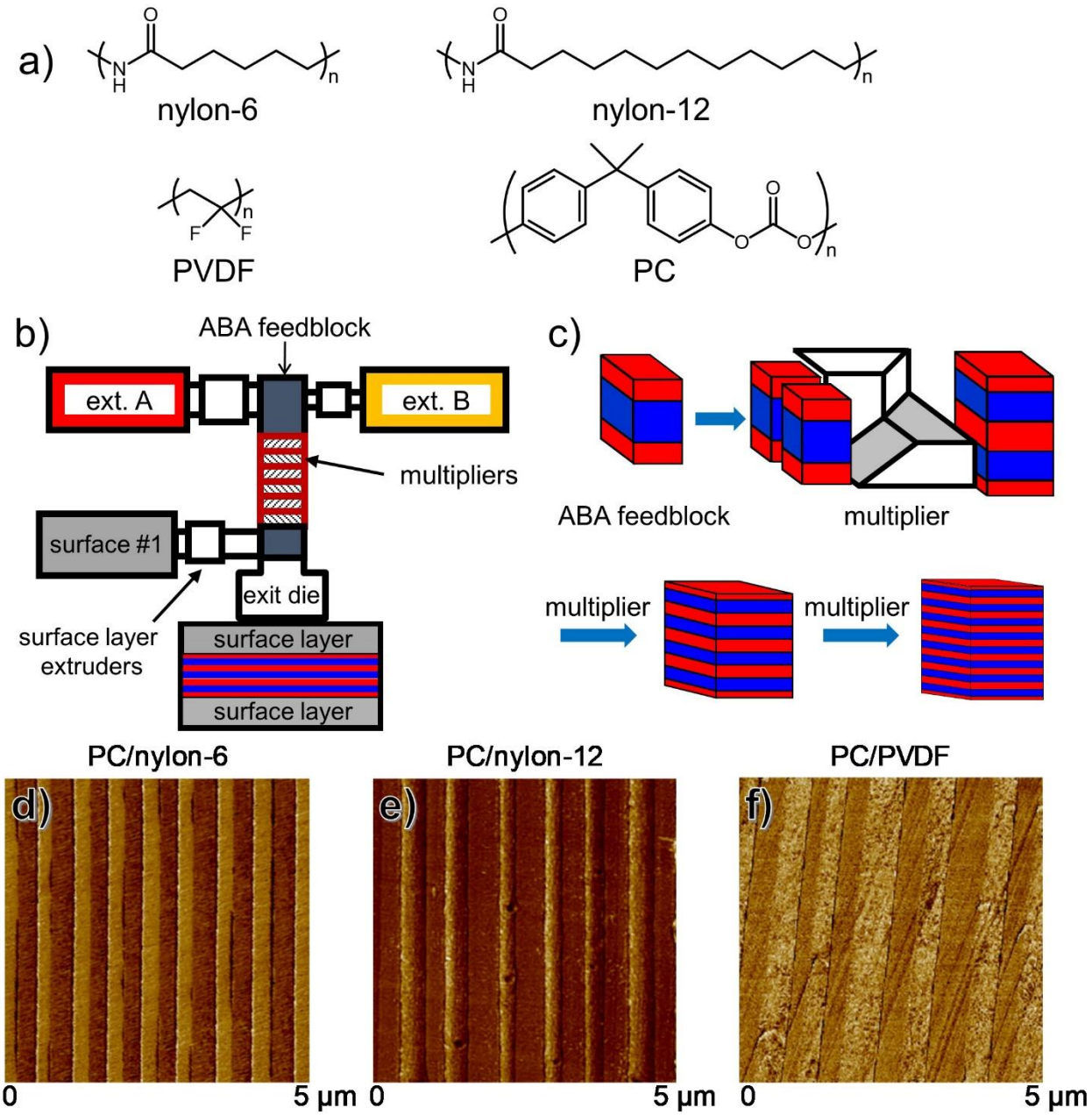

Figure 1. (a) Chemical structures of nylon-6, nylon-12, PVDF, and PC. (b) Schematic of the two-component multilayer coextrusion line using an ABA feedblock and multipliers. (c) Schematic of the layer multiplication. For an ABA feed layer, four multiplication processes are needed to produce a 33-layer film. (d) Tapping-mode AFM phase images of microtome-polished cross-sections for (A) PC/nylon-6, (B) PC/nylon-12, and (C) PC/PVDF 50/50 33L films.

Experimental Section

Materials. PC resin, Makrolon 2207, was purchased from Covestro. Nylon-6 resin, Ultramid B3601, was purchased from BASF. Nylon-12 resin, Grilamid L20 GHS, was purchased

from EMS-Grivory. PVDF resin, Solef® 6010, was purchased from Solvay. All polymer resins were thoroughly dried before melt processing. The chemical structures of nylon-6, nylon-12, PVDF, and PC are shown in Figure 1.

Coextrusion of PC/Nylon and PC/PVDF MLFs. Multilayer coextrusion was conducted using the melt coextrusion lines at both CWRU and PolymerPlus, LLC.[19] First, melt viscosities of PC, nylon-6, nylon-12, and PVDF were determined using a Kayeness Galaxy 1 melt flow indexer under a low shear condition (10 s^{-1}). By matching the melt viscosities, the coextrusion temperature was determined: PC/nylon-6 at 230 °C, PC/nylon-12 at 250 °C, and PC/PVDF at 230 °C, respectively (see Figure S1 in the Supporting Information). The schematic of multilayer coextrusion is shown in Figure 1b. An example for the fabrication of a 50/50 vol./vol. MLF is given below. Briefly, an ABA trilayer feedblock with an A/B/A ratio being 25/50/25 was used to stack the A (PC) and B (nylon-6, nylon-12, or PVDF) components into three layers. The volume ratio between the A and B components was 50/50. After four multiplications (Figure 1c), a 33L [i.e., A′$(BA)_{15}$BA′] film was obtained with both surface A′ layers having half the thickness as the inner A layers. In this work, PC was chosen to be the A/A′ layers for the MLF fabrication. Before exit, two sacrificial low-density polyethylene (LDPE) layers were laminated onto the MLF to avoid damage, reduce surface defects, and keep uniform layer thicknesses. These sacrificial LDPE layers were removed prior to subsequent film characterization. After exit, the MLF was collected using a chiller roll set at 60 °C. The final MLF thickness was controlled to be around 10 μm by adjusting the uptake speed. In the same multilayer coextrusion way, the PC, nylon-6, nylon-12, and PVDF control films were also fabricated with both A and B components being the same polymer.

Film-Level Characterization. To observe the layer structure in the PC/nylon MLFs, we

embedded samples in standard epoxy, which was cured at room temperature overnight. A flat and smooth cross-section of the embedded film was obtained by microtome-polishing at -120 °C using a Leica Microsystem EM FC6 ultramicrotome. Layer continuity and uniformity of the films were characterized using atomic force microscopy (AFM). Phase and height images of the cross-sections were recorded using a Nanoscope IIa Multimode scanning probe (Digital Instruments). AFM was operated using the tapping mode at room temperature.

Thermal properties of the MLFs were measured using a Q2000 differential scanning calorimeter (DSC, TA Instruments). The instrument was calibrated with indium and tin standards. The heating and cooling rates were 10 °C/min and the sample weight was ca. 3 mg.

Dynamic mechanical properties of the MLFs were characterized using a TA DMA Q800 dynamic mechanical analysis (DMA, TA Instruments). The DMA tests were carried out in a tensile mode at a heating rate of 3 °C/min. The testing frequency was 1 Hz.

Two-dimensional (2D) wide-angle X-ray diffraction (WAXD) patterns were collected at the 11-BM Complex Materials Scattering (CMS) beamline of the National Synchrotron Light Source II (NSLS-II), Brookhaven National Laboratory. The monochromatized X-ray wavelength was λ = 0.0918 nm. An in-vacuum CCD (Photonic Science) detector was used for WAXD experiments. The distance between the sample and detector was 23.5 cm for WAXD, which were calibrated using silver behenate with the first-order reflection at a scattering vector of q = 1.076 nm^{-1}. The data acquisition time for each WAXD pattern was 10 s.

Conventional broadband dielectric spectroscopy (BDS) measurements were carried out on a Novocontrol Concept 80 broadband dielectric spectrometer to investigate the frequency- and temperature-dependent dielectric behavior for as-extruded multilayer films at a low voltage of 1 V_{rms} (i.e., root-mean-square voltage). After drying at 60 °C for 24 h, both sides of the film sample

were coated with 10 nm thick gold as electrodes. The electrode diameter was 10 mm (area = 78.5 mm^2). For frequency-scan BDS measurements, real and imaginary relative permittivities (ε_r' and ε_r'') in the range of 10^{-2}–10^6 Hz were measured at a constant temperature. For temperature-scan BDS measurements, the sample was heated from 20 to 250 °C at a rate of 2 °C/min. During the heating processes, ε_r' and ε_r'' were recorded in real time at different frequencies.

D-E loops were measured using a Radiant Technology Premiere II ferroelectric tester at a frequency of 10 Hz using a sinusoidal wave function. Gold electrodes (10 nm thick) were sputter-coated on both sides of the film with a diameter of 2.5 mm. Samples were immersed in a silicone oil bath to avoid corona discharge in air. The maximum electric field was increased stepwise at increment of 50 MV/m until breakdown of the film. High temperature tests were performed using a temperature-controlled heating stage, Arex-6 Conn.Pro System (Chemglass). The discharged energy density ($U_{e,dis}$) and the hysteresis loss% could be calculated based on the area of D-E loop, following previous reports.[20]

Breakdown strength measurements were carried out using a plane-plane electrode geometry. The films were coated with gold electrode on both sides. The diameter of the electrodes was 2.5 mm and the thickness of the electrodes was ca. 10 nm. Samples were immersed in a silicone oil bath to avoid corona discharge in air. A voltage ramp of 500 V/s was applied to the coated films until electrical breakdown using a Quadtech Guardian 20 kV HiPot tester. Thirty repeats were measured for each sample and the breakdown field was plotted using Weibull analysis. From the analysis, the breakdown value (E_b) at 63.2% failure probability was taken as the breakdown strength.

2.4. Capacitor-winding and characterization

For capacitor-winding, the PC/nylon-12 70/30 (vol./vol.) 33L film was scaled up by PolymerPlus, LLC using a similar MLF coextrusion line to obtain 3000 m long and 0.3 m wide film on a roll. The nominal film thickness was 8 μm. A standard metallization scheme was proposed by SBE with 20 Ω/sq. flat aluminum over the active region of the film and a heavy edge of <5 Ω/sq. of zinc/aluminum to allow for electrical connection to the end spray.

A total of seven samples were made using the best quality MLF rolls, i.e., wrinkle-free and uniform thickness. The sample windings were wound on standard 1" cores to a diameter of 72 mm, targeting a nominal capacitance of 30 μF. The windings were then sprayed with Zn using the standard SBE recipe, and the picture of these seven samples are shown in Figure S2. The samples were then subject to an initial 50 V "pre-clearing" prior to thermal curing at 125 °C for 1 h. Capacitance and dissipation factor (tanδ) measurements for initial samples, 50 V pre-cleared samples, and 125 °C cured samples are provided in Table S1 in the Supporting Information. The average capacitance was 21-22 μF and tanδ was around 0.012.

These MLF capacitors were tested to monitor self-healing events using the circuit in Figure S3. The DC voltage was applied to the capacitor under test (DUT) through a 50 kΩ resistor. The capacitor voltage was monitored using a digital voltmeter and a digital oscilloscope. This setup provided a measurement of the DC leakage current through the capacitor sample via the known voltage drop across the 50 kΩ resistor. The time base could be selected to observe the voltage increase from zero and thus note when any events started to occur. The oscilloscope recorded small voltage dips that indicated a local fault was occurring in the capacitor. The parts were then subject to a stepwise voltage stress test up to 700 V for 1 min with no evidence of any clearing or failures. Finally, the capacitors were stepwise stress-tested to failure while monitoring

self-healing events.

Results and Discussion

Preparation and Morphology of PC/Nylon MLFs. Figure S1 shows the melt viscosities for PC, nylon-6, nylon-12, and PVDF under a shear rate of 10 s^{-1} at different temperatures. Note that this shear rate was similar to that in the single-screw extruders, which was used in the multilayer coextrusion process. From this result, the viscosity-matching temperatures were determined: PC/nylon-6 at 230 °C, PC/nylon-12 at 250 °C, and PC/PVDF at 230 °C. Using these melt-processing conditions, PC/nylon-6, PC/nylon-12, and PC/PVDF 50/50 33L films were successfully fabricated. Here, we chose PC layers at both surfaces of the MLF to avoid direct contacts of metal electrodes with the polar polymers in capacitors, because it had been reported that electrochemical reactions could take place for metal electrodes in direct contact with polar PVDF[21] and nylons.[22] The film integrity and layer structure were visualized by AFM study of the cross-sections of the MLFs. Figures 1d-f show the tapping-mode AFM phase images of the microtome-polished cross-sections for PC/nylon-6, PC/nylon-12, and PC/PVDF MLFs. At room temperature, the glassy PC has a higher modulus than semicrystalline nylon-6, nylon-12, and PVDF. Therefore, PC layers appeared to be brighter in the AFM phase images. From these results, it was clear that these MLFs contained a layered structure with relatively uniform thicknesses.

Crystalline Structure and Orientation Confined in MLFs. Crystallinities of nylon-6, nylon-12, and PVDF in the MLFs were studied using DSC. Figure S4 shows the second heating DSC curves for PC/nylon-6, PC/nylon-12, and PC/PVDF 33L films at a heating rate of 10 °C/min. For the PC/nylon-6 33L film, the $T_{m,nylon\text{-}6}$ was 218 °C, and $T_{g,nylon\text{-}6}$ and $T_{g,PC}$ were observed at 52

and 145 °C, respectively. For the PC/nylon-12 33L film, the $T_{m,nylon-12}$ was 176 °C, and $T_{g,nylon-12}$ and $T_{g,PC}$ were seen at 42 and 144 °C, respectively. For the PC/PVDF 33L film, the $T_{m,PVDF}$ was 170 °C and $T_{g,PC}$ was seen at 145 °C. From the heat of fusion (ΔH_f) values, the crystallinities for nylon-6, nylon-12, and PVDF in these MLFs were calculated to be 23%, 15%, and 38%, respectively. Here, the heats of fusion ($\Delta H_f°$) for 100% crystalline extended chain crystals of nylon-6, nylon-12, and PVDF were taken as 230, 245, and 104.5 J/g, respectively.[23]

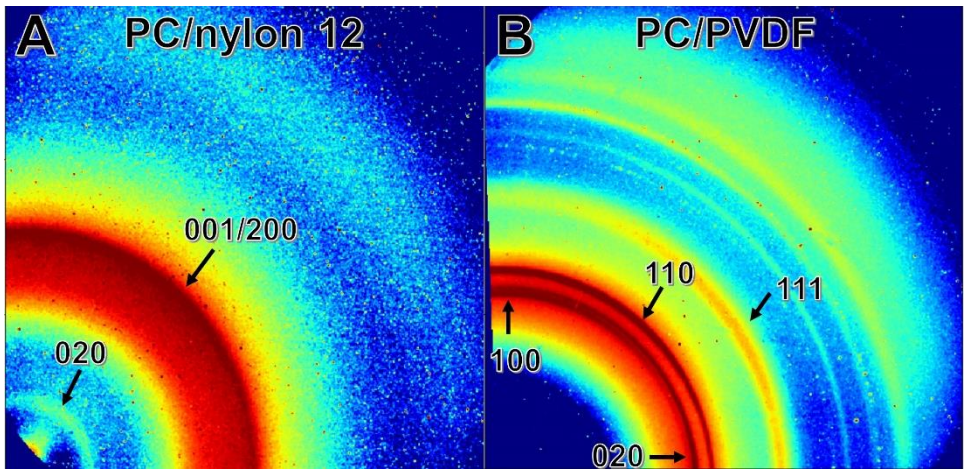

Figure 2. WAXD 2D patterns for as-extruded (A) PC/nylon-12 and (B) PC/PVDF 50/50 33L films. X-ray was directed along the edge-on direction of the MLFs.

The crystalline structure and crystal orientation confined in MLFs were studied by 2D WAXD, as shown in Figure 2. From the WAXD results, nylon-12 in the as-extruded MLFs had the disordered mesomorphic phase with a random crystal orientation. This is consistent with our previous reports on quenched *n*-nylon samples.[24] From the AFM images in Figure 1e, the nylon-12 layers had an average thickness around 400 nm. It was concluded that no confinement effect could be observed for nylon-12 in these nanoconfined layers, possibly due to poor crystal lamellar structures. The situation was different for the PC/PVDF 33L film. As shown in Figure 2B, the $(100)_\alpha$ reflection oriented on the vertical direction, $(020)_\alpha$ reflection oriented on the horizontal

direction, and the $(110)_\alpha$ reflection was seen in the quadrant. This indicated that the α-form PVDF crystals adopted the edge-on crystal orientation when confined in the 400 nm layers of the MLF.[25] Meanwhile, nearly no trace of β-form could be observed in the XRD pattern.

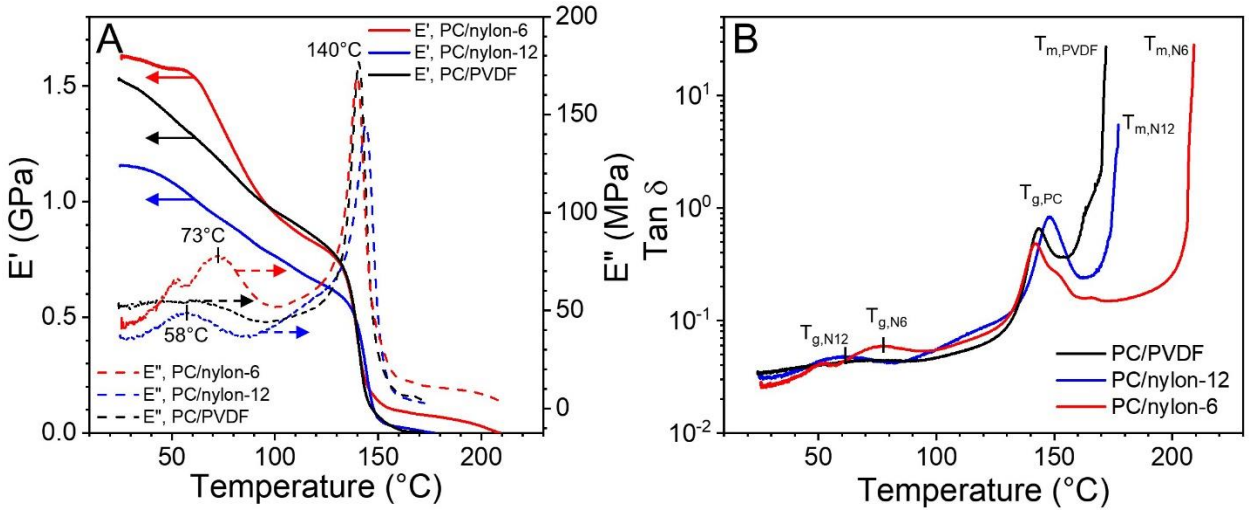

Figure 3. DMA results for (A) storage (E′) and loss (E″) moduli and (B) dissipation factor (tanδ) as a function of temperature for PC/nylon-6, PC/nylon-12, and PC/PVDF 50/50 33L films. The dynamic frequency was 1 Hz.

Dynamic Mechanical Properties of PC/Nylon MLFs. The mechanical properties of various MLFs were studied by DMA. As shown in Figure 3A, the storage moduli (E′) were between 1.1 and 1.6 GPa for these MLFs at room temperature. Upon increasing the temperature, the E′ gradually decreased, especially for PC/nylon-6 and PC/nylon-12 33L films above their T_g around 50 °C. When the temperature reached 130 °C and above, a significant decrease in the E′ was observed for all MLFs, indicating that the MLFs significantly softened around the T_g of PC layers. From the dissipation factor (tanδ) plot in Figure 3B, the dynamic T_g values for nylon-6 and nylon-12 were observed around 75 and 60 °C, respectively. The dynamic T_g values of PC were 140-150 °C. For the PC/nylon-12 and PC/PVDF 33L films, crystal melting started around 170 °C. For the PC/nylon-6 film, crystal melting started around 210 °C. From this DMA study,

we conclude that the upper temperature limit for these MLFs should be around 120 °C, which was determined by the T_g of PC layers.

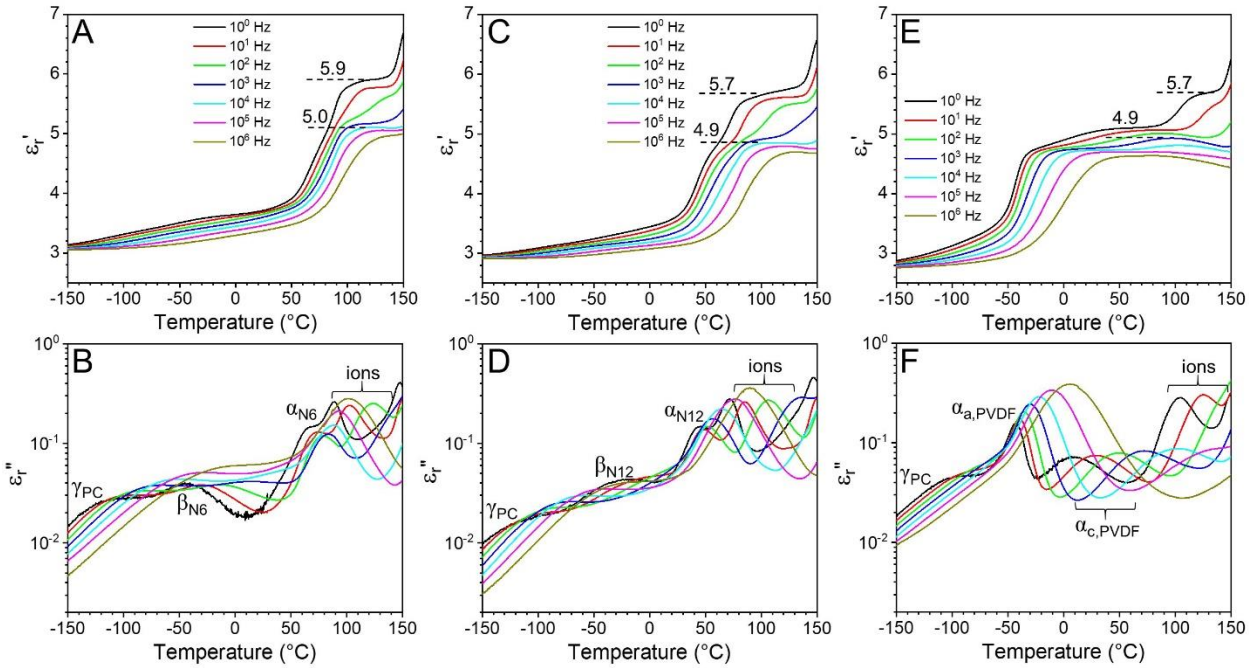

Figure 4. (A,C,E) Real (ε_r') and (B,D,F) imaginary (ε_r'') relative permittivities as a function of temperature for (A,B) PC/nylon-6, (C,D) PC/nylon-12, and (E,F) PC/PVDF films under different frequencies.

Linear Dielectric Properties of PC/Nylon MLFs. Dielectric constant and loss mechanisms in these MLFs were studied by BDS. Various dielectric processes via either relaxation of dipoles or conduction of impurity ions were identified. From the ε_r'' plots in Figures 4B,D [the dissipation factor (tanδ) plots for various MLFs are shown in Figure S5], the γ_{PC} relaxation was observed around -110 °C, which could be attributed to the rotation of the bisphenol A group next to the carbonate group.[26] Around -30 °C, the β relaxation of nylons was observed. This relaxation could be attributed to the segmental motion of nylon samples containing absorbed water, which broke the intermolecular hydrogen-bonding between polyamide chains. Around 60 °C for nylon-6 and 40 °C for nylon-12, the glass (or α) transitions were observed. Above the

glass transition, dielectric loss from conduction of impurity ions could be seen. Note that impurity ions always exist in polar polymers, and even a ppm level of impurity ions could cause significant dielectric loss, especially at high temperatures.[14, 27-28] From Figures 4A,C, dielectric constants for PC/nylon-6 and PC/nylon-12 were around 3.0 at -150 °C. With increasing the temperature above T_g for nylon-6 and nylon-12, dielectric constants significantly increased to around 5.0 for PC/nylon-6 and 4.9 for PC/nylon-12 MLFs. Above the T_g, the apparent dielectric constant increased to 5.9 for PC/nylon-6 and 5.7 for PC/nylon-12 33L films. Note, this increase was not a genuine increase in dielectric constant, but could be ascribed to the conduction of impurity ions, as reported previously.[29-30]

For the PC/PVDF 33L film, dipolar relaxation processes were observed for PVDF, e.g., glass transition ($\alpha_{a,PVDF}$) around -40 °C and $\alpha_{c,PVDF}$ around 0 °C at 1 Hz (Figure 4F).[31-32] These dipolar polarization increased the dielectric constant from ~2.8 at -150 °C to 5.1 around room temperature (Figure 4E). In addition, impurity ion conduction was observed above 90 °C at 1 Hz, which increased the apparent dielectric constant to 5.7. Comparing the genuine dielectric constants for these MLFs, a similar value around 5.0 could be obtained, when the temperature was above T_g, i.e., 75 °C for PC/nylon 33L films and -30 °C for PC/PVDF 33L film.

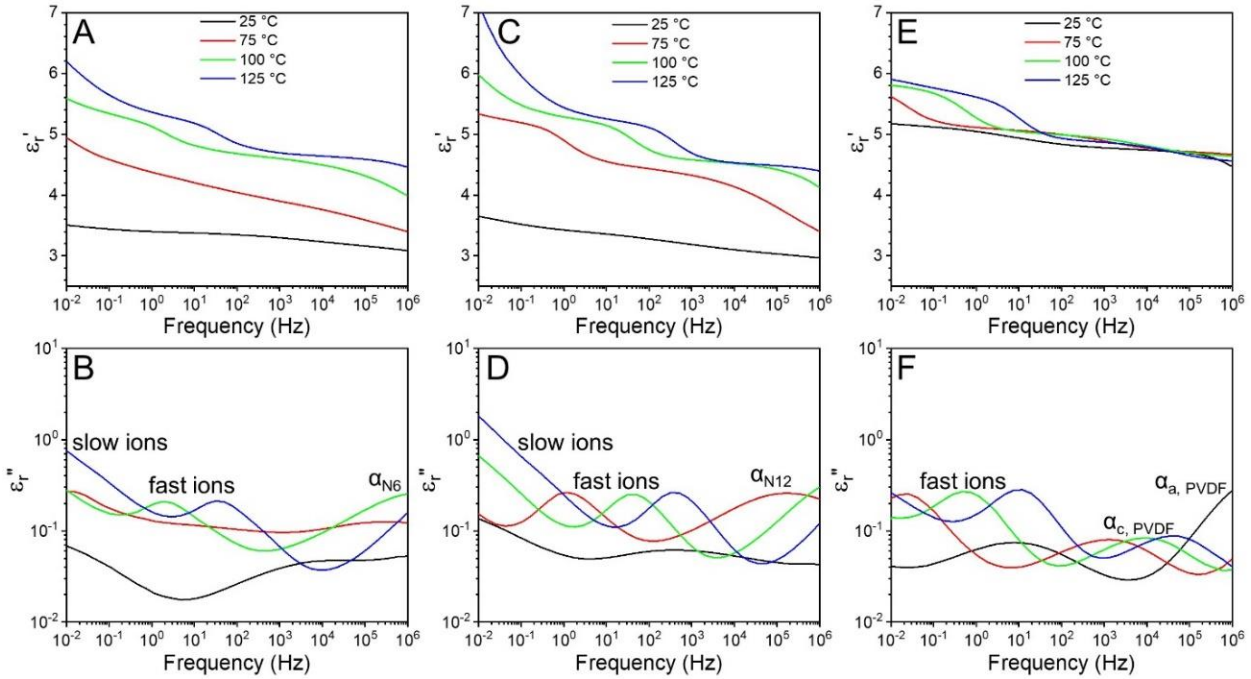

Figure 5. (A,C,E) Real (ε_r') and (B,D,F) imaginary (ε_r'') parts of the relative permittivities as a function of frequency for (A,B) PC/nylon-6, (C,D) PC/nylon-12, and (E,F) PC/PVDF films under different temperatures.

Frequency-scan BDS results for various MLFs are shown in Figure 5. When the temperature was below T_g, PC/nylon MLFs exhibited low dielectric constants over a broad range of frequencies (see Figures 5A,C). The corresponding dissipation factor (tanδ) plots are shown in Figure S6. When the temperature was above T_g, three dielectric events were identified in the ε_r'' plots (Figures 5B,D). At low frequencies, conduction of slow impurity ions (e.g., large Cl^- anions or bigger ions) caused an upturn in ε_r'' with a slope of -1.[28-29] At intermediate frequencies, the peak in ε_r'' were attributed to the conduction of fast impurity ions (e.g., small Na^+ cations).[28-29] At high frequencies, the relaxation of amorphous amide dipoles was observed. For the PC/PVDF 50/50 33L film (Figure 5F), also three dielectric events were observed: i) conduction of fast impurity ions, ii) $\alpha_{c,PVDF}$ (i.e., the wagging motion of CF_2 dipoles along the chain axis),[31-32] and iii) $\alpha_{a,PVDF}$ (i.e., relaxation of amorphous PVDF dipoles). Because the T_g for PVDF was very low (-40 °C), relatively stable dielectric constant was observed between 25 and

125 °C for the PC/PVDF MLF (Figure 5E). From these BDS results, we conclude that PC/nylon MLFs can exhibit high dielectric constants above T_g as a result of orientational polarization of the amorphous amide dipoles.

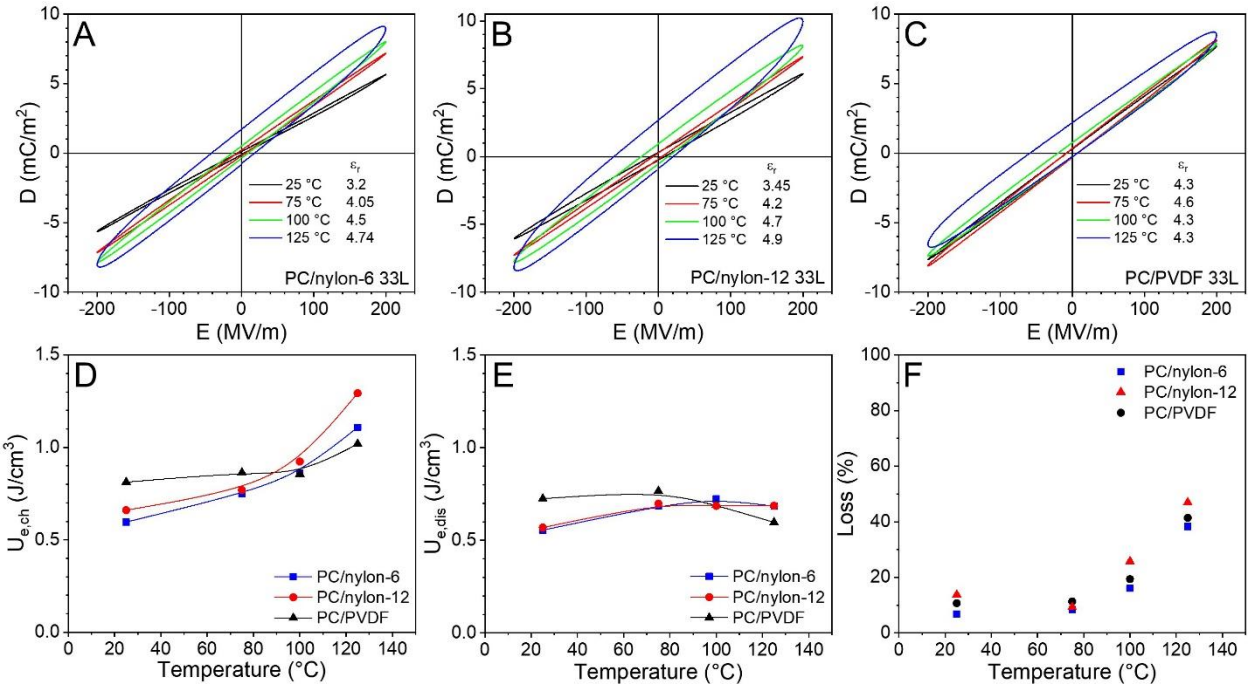

Figure 6. Bipolar D-E loops for (A) PC/nylon-6, (B) PC/nylon-12, and (C) PC/PVDF 50/50 33L films at 25, 75, 100, and 125 °C, respectively. The poling field was 200 MV/m with a 10 Hz sinusoidal waveform. (D) Charged, (E) discharged energy densities, and (F) loss% for PC/nylon-6, PC/nylon-12, and PC/PVDF 50/50 33L films. Results are obtained from D-E loop results in (A-C). Lines are drawn to guide the eyes.

High-Field D-E Loop Study of PC/Nylon MLFs. Bipolar D-E loops were tested for these MLFs, as shown in Figure 6. For PC/nylon-6 and PC/nylon-12 33L films (Figures 6A,B), the D-E loop slope increased with increasing temperature, suggesting an increase in dielectric constant above T_g of nylons around 50 °C. This result is consistent with that seen in the BDS study in Figure 4; however, it is different from the case for the PC/PVDF 33L film (see Figure 6C). Meanwhile, narrow loops were observed when the temperature was 75 °C and below. Above 100 °C, D-E loops became broader. Judging from the asymmetric loop with respect to the origin

point, we could attribute this loop-broadening to AC electronic conduction in the sample at high temperatures (i.e., ≥100 °C), as reported before.[28] When temperature was approaching T_g of PC, homocharge injection from metal electrodes became significant. By reversing the electrode polarity, these homocharges could be neutralized upon injection of the opposite homocharges.[33] As a result, AC electronic conduction near the metal electrode/polymer interfaces caused significant dielectric loss. Similar situation was also seen for PC/PVDF at ≥100 °C (see Figure 6C). To avoid AC electronic conduction, one way is to replace the normal PC with a higher T_g PC to prevent homocharge injection, and this work is currently underway.

From the bipolar D-E loops, charged ($U_{e,ch}$) and discharged ($U_{e,dis}$) energy densities, as well as loss%, could be obtained.[20] Results are summarized in Figures 6D-F. The $U_{e,ch}$ increased with temperature for all MLFs (Figure 6D). The $U_{e,dis}$ decreased for PC/PVDF, whereas it increased and then leveled off above 75 °C for PC/nylon-6 and PC/nylon-12 33L films (Figure 6E). Therefore, the energy loss% increased with increasing temperature (Figure 6F). This increase of dielectric loss was attributed primarily to the AC electronic conduction when the temperature approached the T_g of the outer PC layers, as we discussed above. Again, it is desirable to replace the normal bisphenol A PC with a high T_g PC in order to minimize homocharge injection from metal electrodes at elevated temperatures.

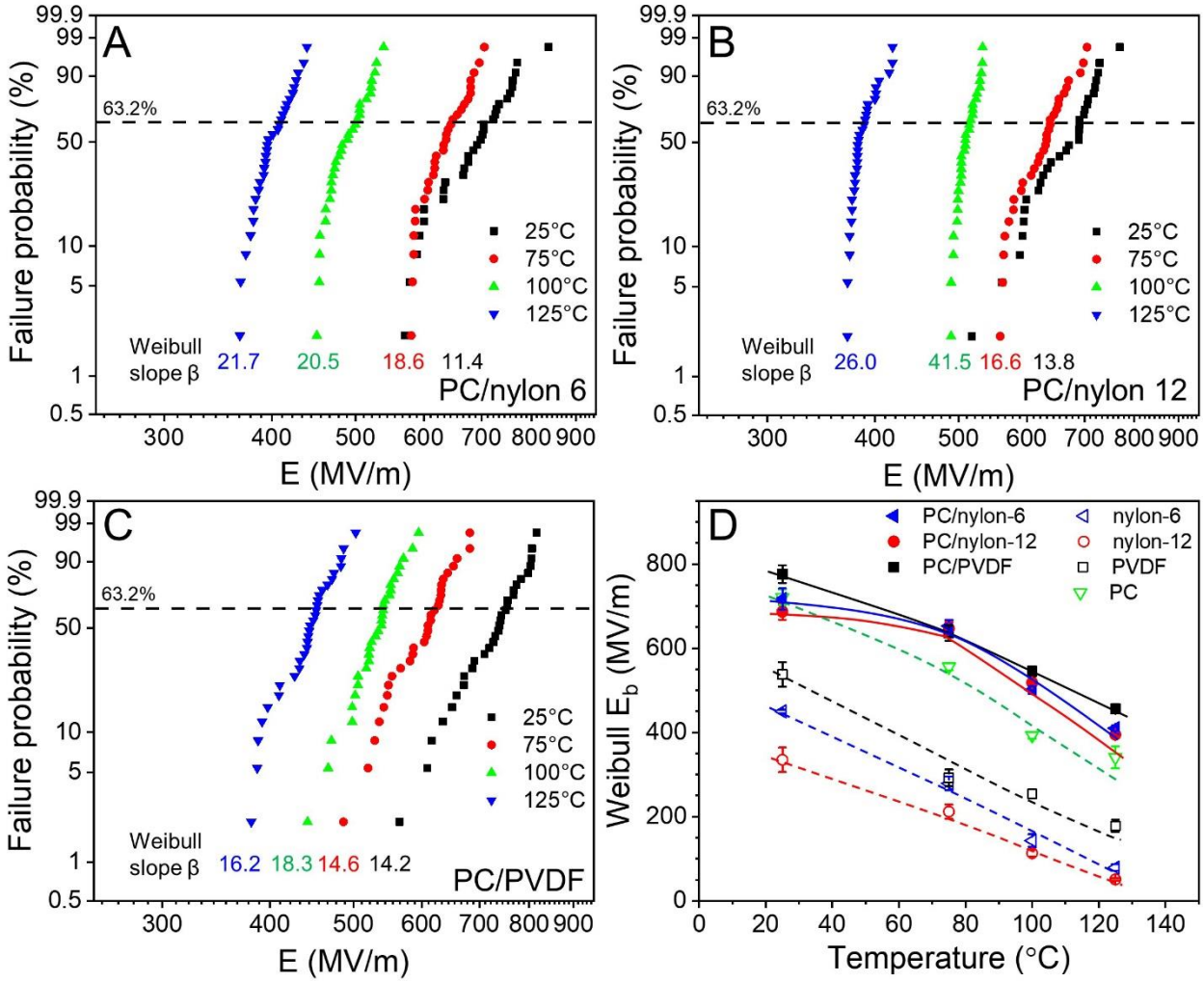

Figure 7. Weibull plots of the first breakdown strength (E_b) distribution for (A) PC/nylon-6, (B) PC/nylon-12, and (C) PC/PVDF 50/50 33L films at different temperatures. (D) Weibull dielectric breakdown strength as a function of temperature for all MLFs. For each data point, 30 samples were tested. Results for control films are also included for comparison.

Weibull Analysis of Dielectric Breakdown Strength of MLFs. Dielectric breakdown strengths for the MLFs were studied using Weibull analysis (Figures 7A-C), and results are summarized in Figure 7D. Upon increasing the temperature, the Weibull E_b at 63.2% failure possibility gradually decreased for all films (including the control films). Intriguingly, the E_b values for all MLFs appeared to be always higher than those of the respective control films above 75 °C. This could be attributed to the interfacial polarization in MLFs, as reported recently.[34-35] Basically, upon electric poling, impurity ions in polar polymers (nylons and PVDF) could migrate

to the interfaces and blocked by the more insulating PC layers to form interfacial charges. These interfacial charges then effectively blocked thermal runaway of hot electrons injected from the metal electrodes. As a result, the breakdown strength would increase for MLFs. This has been observed in other MLF systems, which had a large dielectric contrast in permittivity and bulk conductivity.[36]

Meanwhile, compared with weakly polar PC, highly polar PVDF and nylon control films exhibited much lower E_b values. This could be attributed to potential electrochemical reactions, especially at high electric fields, when the metal electrodes were in direct contact with polar polymers.[21-22] Therefore, in addition to the ferroelectricity in PVDF and nylons, electrochemical reactions under high electric fields were other reasons that prevented neat PVDF or nylon films from being used as neat capacitor films. In this sense, multilayering with PC is an efficient way to make polar polymers suitable for capacitor applications.

Self-Healing Behavior of PC/Nylon MLF Capacitors. Self-healing (or self-clearing) is a critical property for the reliability of metallized film capacitors.[6-7] This essentially allows for the use of polymer films that have some intrinsic defects as manufactured. When current starts to flow through a defect site as a precursor to a breakdown event, the local thin metallization is vaporized, thus removing the defect much like a fuse. The self-healing mechanism is optimized by the selection of metallization material and thickness, and must be able to precede catastrophic faults at elevated temperatures under high voltage stresses. Measurement of self-healing is difficult and for large capacitors can be limited to acoustic detection. Using the circuit in Figure S3, SBE has developed a novel method for monitoring self-healing events in MLF capacitors.

Table 2. Failure Voltage and Self-healing Results for Seven Wound MLF Capacitors.

Serial number	Failure voltage (V)	Self-healing
9284-1	1050	Yes
9284-2	1800	Yes
9284-3	1000	No
9284-4	>2000 (limit of tester)	Yes
9284-5	1300	Yes
9284-6	1850	No
9284-7	1100	No

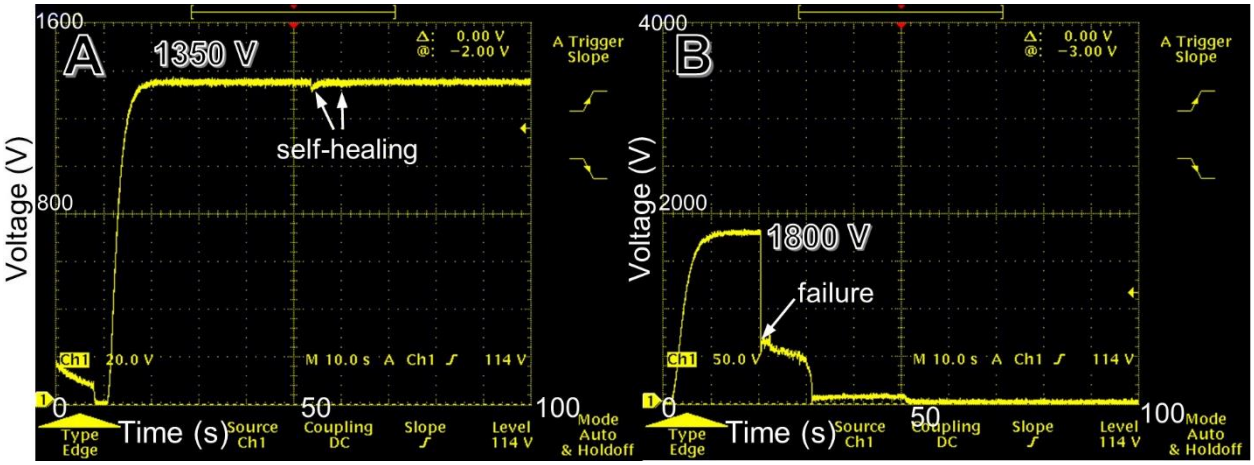

Figure 8. Self-healing test results for the PC/nylon-12 70/30 33L film capacitor, 9284-2. The applied voltages are (A) 1350 V and (B) 1800 V, respectively. Each division in the *x*-axis corresponds to 10 s.

In this study, seven capacitors were wound from metallized MLFs and had an ultimate failure voltage above 1000 V (see Table 2). Note that an 1800 V failure for 8 μm film indicated an electric stress of 225 MV/m for the MLF, which is about half of the 500 MV/m value that is expected for commercial BOPP film capacitors. The failure electric field for wound capacitors appeared to be much lower than the Weibull breakdown strength shown in Figure 7. Several reasons were noted. First, the wound capacitors had a much larger electrode area than the tested MLFs. Second, packaging of MLFs might introduce additional defects at the capacitor level. As shown in Figure 8A, the voltage could recover for sample 9284-2 held at 1350 V (indicated by arrows). Namely, the self-healing mechanism successfully disconnected or "cleared" the metal

connecting the defect. When increasing the voltage to 1800 V, the voltage on the sample collapsed as seen in Figure 8B. Under such a high voltage, self-healing was not able to occur before the defect reached a fault condition. For sample 9284-4, self-healing took place constantly at 2000 V (i.e., ~250 MV/m; see Figure S7), which was the limit of the tester. These results were encouraging, since >50% MLF capacitors showed the self-healing capability without catastrophic drop of the voltage (see Table 2).

In a parallel study, wound PC/PVDF MLF capacitors were also packaged. However, they seldom showed the self-healing capability. We speculate that the chemical structures of aliphatic nylons (e.g., nylon-12) are similar to polyolefins (e.g., BOPP, which are capable of self-healing), except for the amide groups. Under high electric fields, the degradation of aliphatic nylons could be relatively complete. PVDF contains strong C-F bonds. This makes it much more difficult to decompose completely (note that PVDF often forms char upon thermal degradation[37]). As a result, carbonization of PVDF could destroy the self-healing capability.

4. Conclusions

In summary, a new type of high dielectric constant MLFs based on PC and even-numbered nylons has been successfully fabricated via multilayer coextrusion technology. Here, we choose even-numbered nylons rather than odd-numbered nylons, because they do not exhibit ferroelectricity especially at high temperatures. From DMA study, the upper limit temperature for these PC/nylon MLFs was around 120 °C, which was limited by the T_g of PC. At the film level, the PC/nylon MLFs exhibited similar dielectric properties as the PC/PVDF MLF. Above the T_g (~50 °C) of nylons, the PC/nylon MLFs exhibited a relatively high dielectric constant around 5, which was attributed to the dipolar polarization of mobile amorphous amide dipoles. From

Weibull analysis, the PC/nylon MLFs had even higher E_b than the PC control film at >75 °C. Therefore, multilayering with PC was an effective way to significantly enhance the breakdown strength for polar nylons. Finally, the PC/nylon-12 70/30 33L film was scaled up, metallized, and wound into seven ~22 μF capacitors. Unlike wound PC/PVDF MLF capacitors, these PC/nylon-12 MLF capacitors exhibited self-healing behavior when holding under an electrical stress up to 2000 V (~250 MV/m). These results indicate that the PC/nylon MLFs could have a good potential for film capacitor applications.

Supporting Information

The Supporting Information is available free of charge on the ACS Publications website at DOI: xxxxxxxxx.

Melt viscosity of PC, nylon-6, nylon-12, and PVDF, photos of wound MLF capacitors, capacitance and dissipation factor characterization of wound MLF capacitors, schematic circuit for testing the self-healing behavior of wound MLF capacitors, DSC curves for PC/nylon-6, PC/nylon-12, and PC/PVDF MLFs, temperature- and frequency-scan BDS dissipation factor plots for various MLFs, self-healing result for a wound MLF capacitor 9284-4.

Author information

Corresponding Author

*E-mail: (L. Zhu) lxz121@case.edu.

ORICD

Lei Zhu: 0000-0001-6570-9123

Notes

The authors declare no competing financial interest.

Acknowledgments

This work was supported by National Science Foundation via the Partnerships for Innovation: Accelerating Innovation Research – Technology Transfer Program (IIP-1640701). This research used the 11-BM CMS beamline of National Synchrotron Light Source-II (NSLS-II), Brookhaven National Laboratory (BNL), a U.S. Department of Energy User Facility operated for the Office of Science by BNL under contract No. DE-SC0012704.

References

1. Husain, I., *Electric and Hybrid Vehicles: Design Fundamentals*; CRC Press: Boca Raton, 2010, 274 pages.
2. Setter, N.; Colla, E., *Ferroelectric Ceramics: Tutorial Reviews, Theory, Processing, and Applications*; Birkhäuser: Boston, 1993, 380 pages.
3. Li, J.; Li, F.; Xu, Z.; Zhang, S., Multilayer Lead-Free Ceramic Capacitors with Ultrahigh Energy Density and Efficiency. *Adv. Mater.* **2018**, *30*, 1802155.
4. Simon, P.; Gogotsi, Y., Materials for Electrochemical Capacitors. *Nat. Mater.* **2008,** *7*, 845-854.
5. Nishino, A., Capacitors: Operating Principles, Current Market and Technical Trends. *J. Power Sources* **1996,** *60*, 137-147.
6. Sarjeant, W. J.; Zirnheld, J.; MacDougall, F. W., Capacitors. *IEEE Trans. Plasm. Sci.* **1998,**

26, 1368-1392.

7. Sarjeant, W. J.; Clelland, I. W.; Price, R. A., Capacitive Components for Power Electronics. *Proc. IEEE.* **2001,** *89*, 846-855.
8. Kim, S. H.; Hong, K.; Xie, W.; Lee, K. H.; Zhang, S.; Lodge, T. P.; Frisbie, C. D., Electrolyte-Gated Transistors for Organic and Printed Electronics. *Adv. Mater.* **2013,** *25*, 1822-1846.
9. Montanari, D.; Saarinen, K.; Scagliarini, F.; Zeidler, D.; Niskala, M.; Nender, C. Film Capacitors for Automotive and Industrial Applications. *Proceedings of CARTS U.S.A. 2009*; Jacksonville, FL, March 30-April 2, 2009.
10. Ho, J.; Jow, T. R. *Characterization of High Temperature Polymer Thin Films for Power Conditioning Capacitors*; Army Research Laboratory: Adelphi, MD, 2009.
11. Tan, D.; Zhang, L.; Chen, Q.; Irwin, P., High-Temperature Capacitor Polymer Films. *J. Electron. Mater.* **2014,** *43*, 4569-4575.
12. Zhang, X.-M.; Liu, J.-G.; Yang, S.-Y., A Review on Recent Progress of R&D for High-Temperature Resistant Polymer Dielectrics and Their Applications in Electrical and Electronic Insulation. *Rev. Adv. Mater. Sci.* **2016,** *46*, 22-38.
13. Li, Q.; Yao, F.-Z.; Liu, Y.; Zhang, G.; Wang, H.; Wang, Q., High-Temperature Dielectric Materials for Electrical Energy Storage. *Ann. Rev. Mater. Res.* **2018,** *48*, 219-243.
14. Baer, E.; Zhu, L., 50th Anniversary Perspective: Dielectric Phenomena in Polymers and Multilayered Dielectric Films. *Macromolecules* **2017,** *50*, 2239-2256.
15. Demeuse, M. T., *Biaxial Stretching of Film: Principles and Applications*; Woodhead Publishing: Oxford, 2011, 273 pages.
16. Schosseler, L., A New Commercial High Temperature Capacitor Dielectric for Power Applications. *Bodo's Power Systems* **2016**, *April*, 50-51.

17. Zhu, L., Exploring Strategies for High Dielectric Constant and Low Loss Polymer Dielectrics. *J. Phys. Chem. Lett.* **2014,** *5*, 3677-3687.

18. Zhang, Z.; Litt, M. H.; Zhu, L., Understanding the Paraelectric Double Hysteresis Loop Behavior in Mesomorphic Even-Numbered Nylons at High Temperatures. *Macromolecules* **2017,** *50*, 5816-5829.

19. Langhe, D.; Ponting, M., *Manufacturing and Novel Applications of Multilayer Polymer Films*; Elsevier: Amsterdam, 2015.

20. Zhu, L.; Wang, Q., Novel Ferroelectric Polymers for High Energy Density and Low Loss Dielectrics. *Macromolecules* **2012,** *45*, 2937-2954.

21. Eberle, G.; Schmidt, H.; Eisenmenger, W., Influence of Poling Conditions on the Gas Emission of PVDF. *IEEE 1993 Annual Report* **1993**, 263-268.

22. Seanor, D. A., Electronic and Ionic Conductivity in Nylon 66. *J. Polym. Sci., Part A2* **1968,** *6*, 463-477.

23. Wunderlich, B., *Thermal Analysis of Polymeric Materials*; Springer: Berlin, 2005.

24. Zhang, Z.; Litt, M. H.; Zhu, L., Unified Understanding of Ferroelectricity in *n*-Nylons: Is the Polar Crystalline Structure a Prerequisite? *Macromolecules* **2016,** *49*, 3070-3082.

25. Mackey, M.; Flandin, L.; Hiltner, A.; Baer, E., Confined Crystallization of PVDF and a PVDF-TFE Copolymer in Nanolayered Films. *J. Polym. Sci., Part B: Polym. Phys.* **2011**, *49*, 1750-1761.

26. Fried, J. R., Sub-Tg Transitions. In *Physical Properties of Polymers Handbook*; Mark, J. E., Ed.; Springer: New York, 2007; Chapter 13, pp 217-232.

27. Mackey, M.; Schuele, D. E.; Zhu, L.; Baer, E., Layer Confinement Effect on Charge Migration in Polycarbonate/Poly(vinylidene fluorid-*co*-hexafluoropropylene) Multilayered

Films. *J. Appl. Phys.* **2012,** *111*, 113702.

28. Yang, L.; Allahyarov, E.; Guan, F.; Zhu, L., Crystal Orientation and Temperature Effects on Double Hysteresis Loop Behavior in a Poly(vinylidene fluoride-co-trifluoroethylene-*co*-chlorotrifluoroethylene)-*graft*-Polystyrene Graft Copolymer. *Macromolecules* **2013,** *46*, 9698-9711.
29. Huang, H.; Chen, X.; Yin, K.; Treufeld, I.; Schuele, D. E.; Ponting, M.; Langhe, D.; Baer, E.; Zhu, L., Reduction of Ionic Conduction Loss in Multilayer Dielectric Films by Immobilizing Impurity Ions in High Glass Transition Temperature Polymer Layers. *ACS Appl. Energy Mater.* **2018,** *1*, 775-782.
30. Huang, H.; Chen, X.; Li, R.; Fukuto, M.; Schuele, D. E.; Ponting, M.; Langhe, D.; Baer, E.; Zhu, L., Flat-On Secondary Crystals as Effective Blocks To Reduce Ionic Conduction Loss in Polysulfone/Poly(vinylidene fluoride) Multilayer Dielectric Films. *Macromolecules* **2018,** *51*, 5019-5026.
31. Yang, L.; Ho, J.; Allahyarov, E.; Mu, R.; Zhu, L., Semicrystalline Structure Dielectric Property Relationship and Electrical Conduction in a Biaxially Oriented Poly(vinylidene fluoride) Film under High Electric Fields and High Temperatures. *ACS Appl. Mater. Interfaces* **2015,** *7*, 19894-19905.
32. Bachmann, M. A.; Lando, J. B., A Reexamination of the Crystal-Structure of Phase-II of Poly(vinylidene fluoride). *Macromolecules* **1981,** *14*, 40-46.
33. Jow, T. R.; Cygan, P. J., Dielectric Breakdown of Polyvinylidene Fluoride and Its Comparisons with Other Polymers. *J. Appl. Phys.* **1993,** *73*, 5147-5151.
34. Tseng, J.-K.; Tang, S.; Zhou, Z.; Mackey, M.; Carr, J. M.; Mu, R.; Flandin, L.; Schuele, D. E.; Baer, E.; Zhu, L., Interfacial Polarization and Layer Thickness Effect on Electrical

Insulation in Multilayered Polysulfone/Poly(vinylidene fluoride) Films. *Polymer* **2014,** *55*, 8-14.

35. Chen, X.; Tseng, J.-K.; Treufeld, I.; Mackey, M.; Schuele, D. E.; Li, R.; Fukuto, M.; Baer, E.; Zhu, L., Enhanced Dielectric Properties due to Space Charge-induced Interfacial Polarization in Multilayer Polymer Films. *J. Mater. Chem. C* **2017,** *5*, 10417-10426.
36. Mackey, M.; Hiltner, A.; Baer, E.; Flandin, L.; Wolak, M. A.; Shirk, J. S., Enhanced Breakdown Strength of Multilayered Films Fabricated by Forced Assembly Microlayer Coextrusion. *J. Phys. D-Appl. Phys.* **2009,** *42*, 175304.
37. Pan, M.; Yang, L.; Wang, J.; Tang, S.; Zhong, G.; Su, R.; Sen, M. K.; Endoh, M. K.; Koga, T.; Zhu, L., Composite Poly(vinylidene fluoride)/Polystyrene Latex Particles for Confined Crystallization in 180 nm Nanospheres via Emulsifier-Free Batch Seeded Emulsion Polymerization. *Macromolecules* **2014**, *47*, 2632-2644.

TOC Graphic

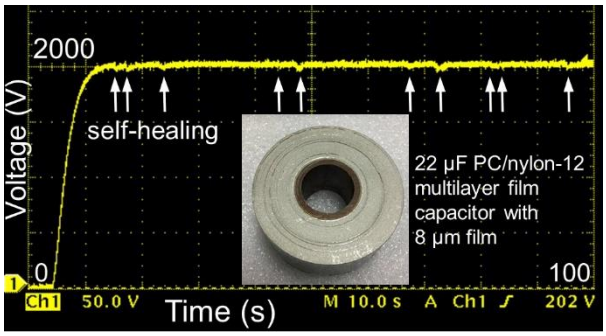
2000
Voltage (V)
self-healing
22 µF PC/nylon-12
multilayer film
capacitor with
8 µm film
0
100
Ch1 50.0 V
Time (s)
M 10.0 s A Ch1 202 V

Supporting Information

High Dielectric Constant Polycarbonate/Nylon Multilayer Films Capacitors with Self-healing Capability

Zhenpeng Li,[†] Xinyue Chen,[†] Ci Zhang,[†] Eric Baer,[†] Deepak Langhe,[‡] Michael Ponting,[‡] Michael Brubaker,[§] Terry Hosking,[§] Ruipeng Li,[#] Masafumi Fukuto,[#] and Lei Zhu*[,†]

[†] *Department of Macromolecular Science and Engineering, Case Western Reserve University, Cleveland, Ohio 44106-7202, United States*
[‡] *PolymerPlus, LLC, 7700 Hub Parkway, Valley View, Ohio 44125, United States*
[§] *SBE, Inc., 81 Parker Road, Barre, Vermont 05641-9106 United States*
[#] *National Synchrotron Light Source II, Brookhaven National Laboratory, Upton, New York 11973, United States*

* Corresponding author. E-mail address: lxz121@case.edu (L. Zhu).

I. Melt Viscosity of PC, Nylon-6, Nylon-12, and PVDF

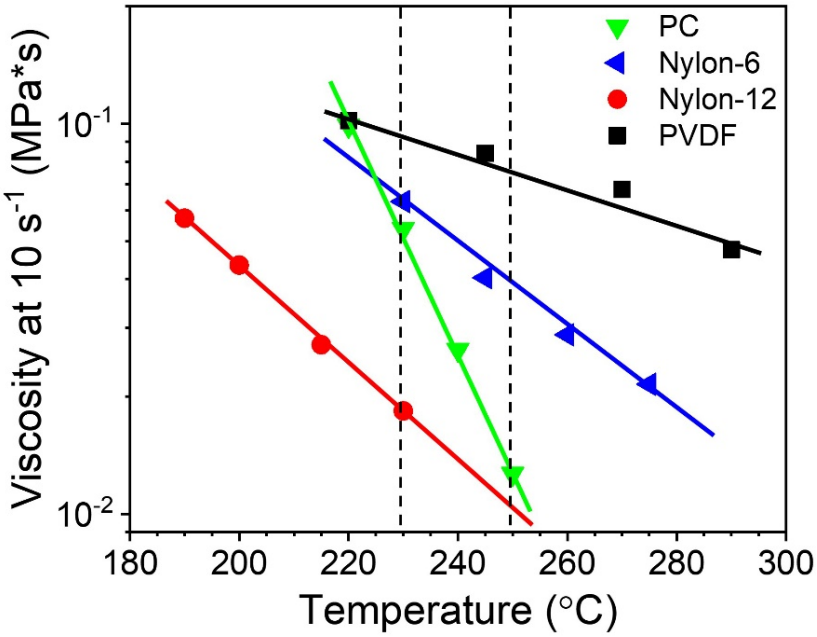

Figure S1. Melt viscosity at 10 s^{-1} as a function of temperature for PC, nylon-6, nylon-12, and PVDF. This plot was used to determine the coextrusion temperature window, which was between 230 and 250 °C.

II. Photos of Wound Multilayer Film Capacitors

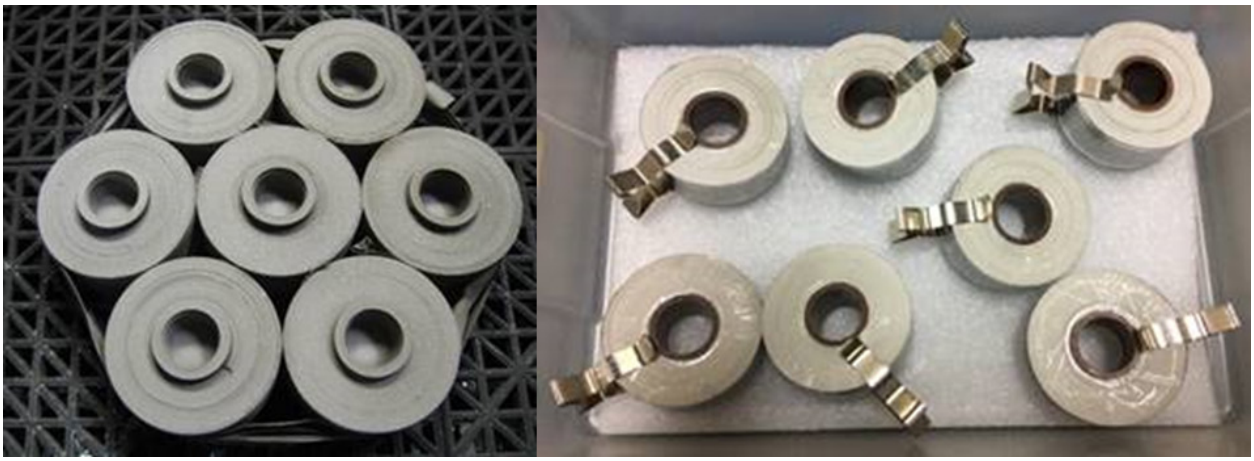

Figure S2. Wound capacitors (target capacitance ~30 µF) from metallized PC/nylon-12 50/50 33L film (ca. 8 µm) after end-spray with Zn.

III. Capacitance and Dissipation Factor Characterization of Wound MLF Capacitors

Table S1. Capacitance and Dissipation Factor (DF) for Wound MLF Capacitors after End Spray, Pre-clearing at 50 V, and Post-cure at 125 °C.

Sample No.	Pre-cure cap. (μF)	Pre-cure DF	Pre-cure 50 V clear cap. (μF)	Pre-cure 50 V clear DF (μF)	Post-cure cap. (μF)	Post-cure DF (μF)
9284-1	22.2	0.010	22.2	0.010	22.4	0.012
9284-2	21.8	0.010	21.8	0.010	22.0	0.011
9284-3	21.9	0.010	21.9	0.010	22.0	0.011
9284-4	21.6	0.010	21.6	0.010	21.9	0.012
9284-5 *	25.4	0.059	21.3	0.057	21.5	0.012
9284-6 *	77.1	1.616	21.3	0.010	21.6	0.012
9284-7	21.1	0.010	21.1	0.010	21.2	0.012

* Note that samples 9284-5 and 9284-6 appear to have end spray short circuits across the margin prior to pre-clearing at 50 V.

IV. Schematic Circuit for Testing the Self-healing Behavior of Wound MLF Capacitors

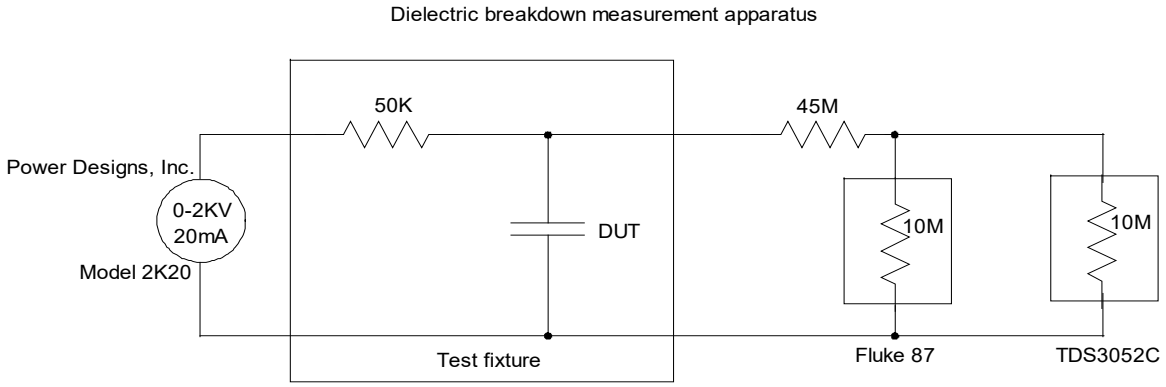

Figure S3. Schematic circuit for testing the self-healing behavior for PC/nylon-12 MLF capacitors.

V. DSC Curves for PC/Nylon-6, PC/Nylon-12, and PC/PVDF MLFs

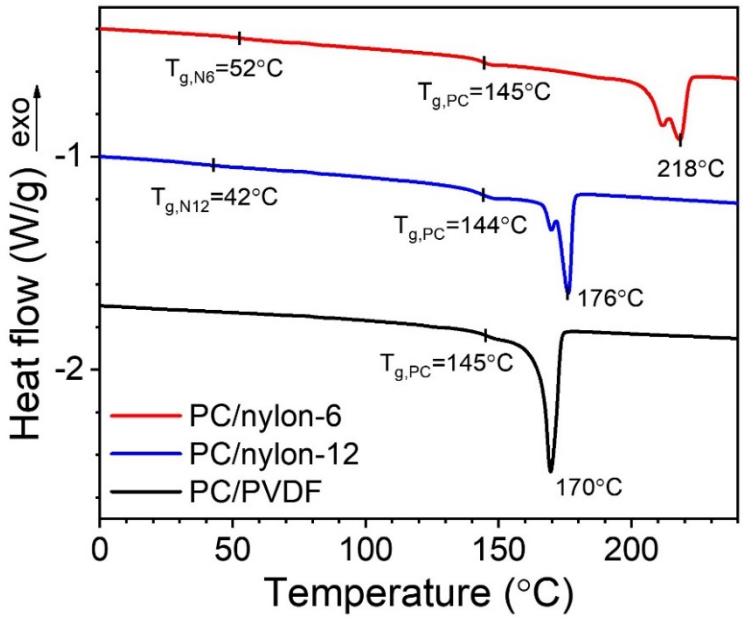

Figure S4. Second heating DSC curves for PC/nylon-6, PC/nylon-12, and PC/PVDF 50/50 33L films. The heating rate was 10 °C/min.

VI. Temperature-scan Dissipation Factor Plots for Various MLFs

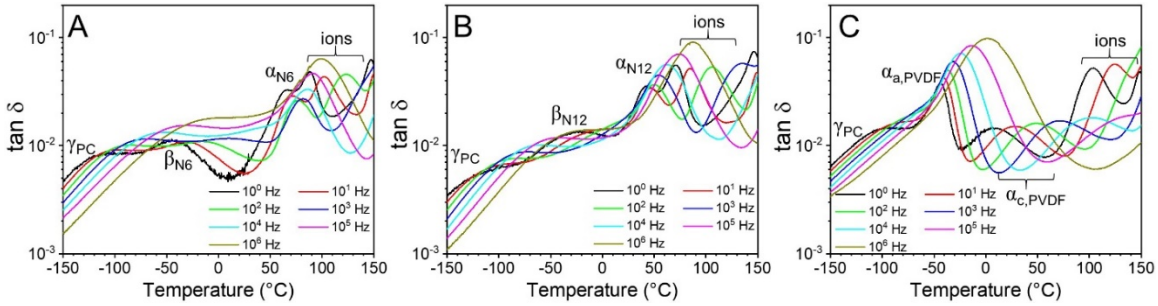

Figure S5. Temperature-scan dissipation factor (tanδ) plots for (A) PC/nylon-6, (B) PC/nylon-12, and (C) PC/PVDF 50/50 33L films at various frequencies.

VII. Frequency-scan Dissipation Factor Plots for Various MLFs

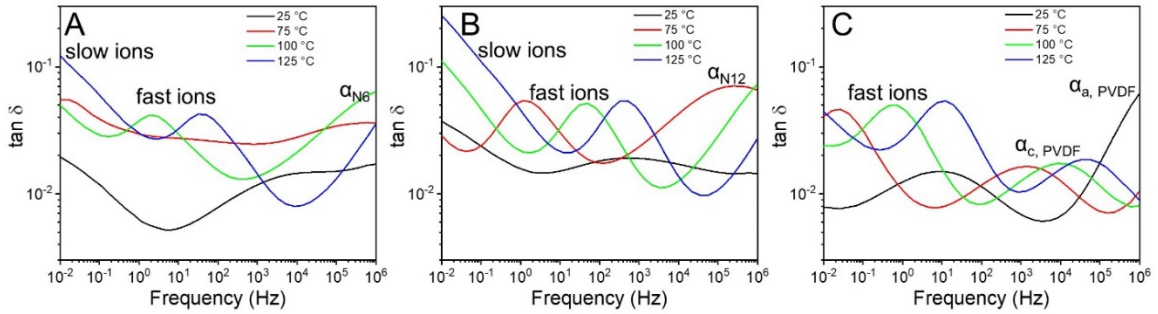

Figure S6. Frequency-scan dissipation factor (tanδ) plots for (A) PC/nylon-6, (B) PC/nylon-12, and (C) PC/PVDF 50/50 33L films at various temperatures.

VIII. Self-healing Result for Wound MLF Capacitor 9284-4

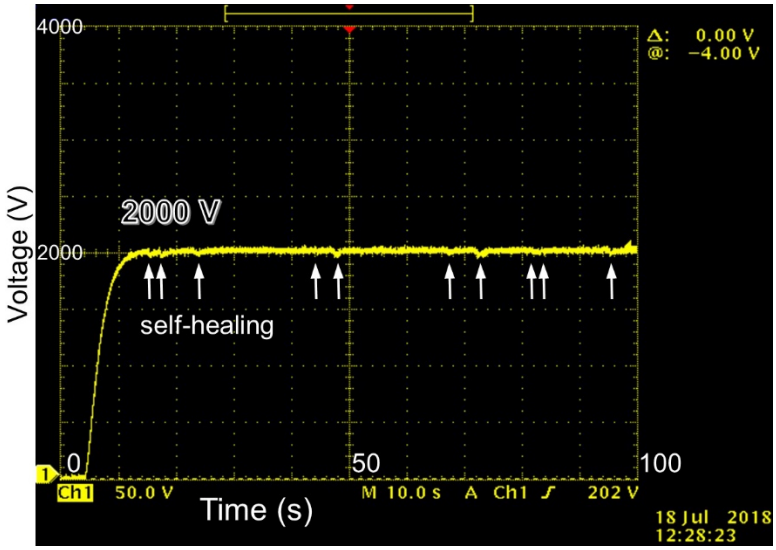

Figure S7. Self-healing test results for the PC/nylon-12 70/30 33L film capacitor, 9284-4. The applied voltage is 2000 V. Each division in the *x*-axis corresponds to 10 s. Clear self-healing events are indicated by arrows. There were other self-healing events audible but not clearly seen in the curve. This capacitor sample did not fail at 2000 V, which is the limit of the tester.